Soils and Rocks
An International Journal of Geotechnical and Geoenvironmental Engineering
www.soilsandrocks.com
ISSN 1980-9743
ISSN-e 2675-5475

Evaluation of breach and rheological parameters for self-rescue zone (ZAS) definition of mining dams

Pedro de Carvalho Thá[1,2#], André Luiz Tonso Fabiani[2]

Article

Keywords
Tailings dam breach analysis
Tailings rheology
Non-Newtonian fluid behavior

Abstract

Recent tailings dam failure in Brazil resulted in significant social, environmental and economic impact. Following the failures, Brazilian regulation changed and demanded tailings dam breach analysis to consider Non-Newtonian fluid behavior, where applicable. However, in addition to rheology, other variables such as failure mode, breach hydrograph and Manning coefficient also influence tailings runout. The objective of the present study is to evaluate the influence of rheological and breach parameters (including failure mode) on tailings runout and, especially, on self-rescue zone (ZAS) definition. The study evaluated tailings breach runout for four iron ore tailings dams located in Brazil. Runout simulations considered different peak flow hydrographs for overtopping and piping, through Monte Carlo analysis. For liquefaction a single hydrograph was considered. Different combinations of hydrographs and rheology were evaluated, as well as Newtonian behavior (water parameters). Rheological parameters were taken specifically for one dam and from a database of 1162 vane rheometer tests in iron ore tailings and sediments for other three dams. Manning coefficient variation was also evaluated. Results were evaluated for four hydraulic variables along downstream path: frontal wave arrival time, time to peak, maximum wave velocity and height. Comparison of results through Kruskall-Walis test indicated that for most of the cases rheological parameters and Manning coefficient variation produced similar results. Peak flow hydrographs influenced results significantly. Self-rescue zone downstream extent was only influenced by liquefaction failure mode. Lateral extent of self-rescue zone was only slightly influenced by rheology variation but was influenced by peak flow hydrographs.

1. Introduction

A tailings dam failure is characterized as a physical breach of the dam followed by uncontrolled and typically sudden and catastrophic release of stored materials (water, tailings, etc.) (CDA, 2021). Subsequent flow of released material can result in substantial environmental, social and economic impacts (Ghahramani et al, 2024). Due to potential impacts, predicting tailings dam breach runout is essential for safety management and is part of the Global Industry Standard on Tailings Management - GISTM (Global Tailings Review, 2020).

In recent years, two large tailings dams failed in Brazil (Corrego do Feijão Dam in 2019 and Fundão Dam in 2015), resulting in catastrophic consequences. Despite the catastrophic consequences, these failures are not isolated events. Rana et al. (2021) presents a review of 63 tailings dam runout from 1965 to 2020. The study indicates that outflow volume in excess of 1 hm^3 have occurred at a mean recurrence interval of 2–3 years during the period. Only in Brazil, Fernandes (2020) indicates 12 failures of tailings dams.

Tailings dams fail for different reasons. Statistical analysis of tailings dams failure indicate slope instability, overtopping and piping as the most frequent failure modes (Piciullo et al., 2022; Stark et al., 2022). These findings are in accordance with statistics presented in Icold Bulletin 188 for earth dams (ICOLD, 2025). Gildeh et al. (2021) also indicate the same failure modes as being the most frequent for tailings dams, but separate liquefaction from other instability cases and highlights it as a frequent failure mode.

After the failure of Corrego do Feijão Dam in 2019, regulatory agencies in Brazil applied measures to increase safety of existing tailings dams. Among these measures, one of the most important is resolution ANM 95/2022 (ANM, 2022). Tailings dam breach analysis (TDBA) is mandatory and should consider rheological parameters for tailings and the failure mode which lead to most severe downstream consequence, regardless probability of occurrence. If

#Corresponding author. E-mail address: pedro.tha@gmail.com
[1]Intertechne Consultores, Curitiba, PR, Brasil.
[2]Universidade Federal do Paraná, Programa de Pós-graduação em Engenharia de Recursos Hídricos e Ambiental, Curitiba, PR, Brasil.

Submitted on July 31, 2026; Final Acceptance on September 19, 2026; Discussion open until February 28, 2027.
Editor: Renato P. Cunha
https://doi.org/10.28927/SR.2026.015626

This is an Open Access article distributed under the terms of the Creative Commons Attribution license (https://creativecommons.org/licenses/by/4.0/), which permits unrestricted use, distribution, and reproduction in any medium, provided the original work is properly cited.

liquefaction is possible, TDBA should consider maximum dam and reservoir volume possible to be mobilized.

CDA (2021) presents specific guidance for TDBA and there is guidance applied to all kinds of dams (ABNT, 2024; FEMA, 2013). Regardless of stored material (tailings, sediment, fluid, etc.), all dam breach analysis requires the definition of breach hydrograph to be routed downstream. Prediction of outflow hydrograph is generally divided into two classes: parametric and physically based (Walsh et al., 2021). Parametric definition is based on observation of historical failure cases to predict breach parameters (e.g., MacDonald & Langridge-Monopolis, 1984; Von Thun & Gillette, 1990; Froehlich, 1995, 2008, 2016; Xu & Zhang, 2009). According to West et al. (2018), Froehlich (1995, 2008) methods generally provide reasonable breach parameters and is considered the standard method for breach parameters prediction. Nonetheless, Froehlich (1995, 2008) propositions were developed for water flow and for piping and overtopping failure modes. Application to tailings have several limitations, as well as physically based models. One way to address limitations, when considering piping or overtopping as credible failure modes, is to define breach hydrograph by the parameters combination resulting in a peak discharge with 5% of exceedance probability (Martin et al., 2022).

CDA (2021) guidelines for TDBA, as well as resolution ANM 95/2022 (ANM, 2022) and NBR 17188 (ABNT, 2024) indicate that breach runout analysis should consider rheological parameters for outflow volume, if applicable. It leads to another set of parameters to be considered on the runout analysis. There are different rheological models which could be used to simulate tailings runout (e.g., Bingham, Voellmy, quadratic, etc.). To evaluate the effect of rheological models in tailings runout, Ghahramani et al. (2022) back-analyzed two tailings dam runout using four different numerical models (DAN3D, MADflow, FLO-2D, and FLOW-3D) with three different rheological models. Results indicated that all four models were able to properly reproduce the tailings runout. However, multiple sets of rheological parameters resulted in very similar output results. Ghahramani et al. (2024) applied the first-order second-moment (FOSM) methodology to a database of 11 back-analyzed historical tailings flows to evaluate uncertainties in runout and to identify key factors contributing to the variability of results. A single numerical model was used (HEC-RAS). Input parameters evaluated were total released volume, Manning coefficient, yield stress, viscosity, breach width and breach formation time. They found that the total released volume is among the top contributors to the sensitivity of modelled inundation area and maximum flow depth, while surface roughness is among the top contributors to the sensitivity of modelled maximum flow velocity and flow front arrival time.

Among the requirements presented in resolution ANM 95/2022 (ANM, 2022) and NBR 17188 (ABNT, 2024), one is to present the runout footprint (flood extent) and to define the self-rescue zone (ZAS). ZAS is defined as the portion of the total runout footprint in which arrival time is 30 minutes or as 10 km in the main downstream channel, whichever gives the longest result. Defining ZAS is particularly important because it is considered susceptible to higher risk for population, since it is considered that public authorities don't have time to take any action. All safety actions in this area (ZAS) have to be taken by the dam owner.

Considering that there are many uncertainties for TDBA analysis and Brazilian regulation requires explicitly tailings rheological parameters to be considered in analysis, the objective of the present study is to evaluate influence of breach and rheological parameters in tailings breach runout. The focus of the study is given to the first 10 km downstream, where ZAS is normally defined. The study evaluates tailings runout for four tailings dams.

2. Materials and methods

2.1 Dams

To evaluate breach and rheological parameters on ZAS delineation, four tailings dams were selected. All dams store iron ore tailings and are located in Brazil. Dams are referred in the present study as B1, B2, B3 and B4. For confidentiality reasons, it is not possible to disclose their real names. According to ICOLD (2011) criteria, all dams are considered big dams, due to maximum height in excess of 15 m. Table 1 summarizes dam's geometry.

2.2 Downstream topography

The downstream topography used for all dams is composed by DTM (digital terrain model) of 1 m resolution. All DTM were derived from laser airborne surveys, with points density compatible with 1:5,000 scale and complying to PEC A (Brasil, 1984).

Table 1. Summary of dams geometry.

Dam	Height (m)	Crest length (m)	Reservoir volume (hm^3)		
			Total	Tailings	Water[(1)]
B1	68	850	66.70	52.20	14.40
B2	62	284	2.82	2.24	0.58
B3	130	860	42.20	38.61	3.59
B4	29	370	1.60	1.14	0.46

[(1)]Water volume up to crest.

Table 2. Expected breach parameters variation based on Froehlich (2008).

Dam	Failure mode	Side slope (Z:1V)	Bottom width (m)	Formation time (hours)
		Av/Min/Max/SD	Av/Min/Max/SD	Av/Min/Max/SD
B1	Overtopping	1.0/0.19/5.38/1.46	64.5/5.0/272.5/48.2	2.42/1.20/5.00/0.64
	Piping	0.7/0.13/3.72/0.91	54.3/5.0/212.4/36.7	2.42/1.1/5.2/0.68
B2	Overtopping	1.0/0.19/5.38/1.46	5.0/5.0/66.5/18.2	0.56/0.3/1.2/0.15
	Piping	0.7/0.13/3.72/0.91	5.0/5.0/54.7/13.9	0.56/0.3/1.2/0.16
B3	Overtopping	1.0/0.19/5.38/1.46	5.0/5.0/180.2/44.3	1.01/0.5/2.1/0.27
	Piping	0.7/0.13/3.72/0.91	5.0/5.0/145.9/33.7	1.01/0.5/2.2/0.28
B4	Overtopping	1.0/0.19/5.38/1.46	9.8/5.0/71.7/14.3	0.88/0.4/1.8/0.23
	Piping	0.7/0.13/3.72/0.91	9.5/5.0/56.6/10.9	0.88/0.4/1.9/0.25

Legend: *Av* = average; *Min* = minimum, *Max* = maximum; *SD* = standard deviation.

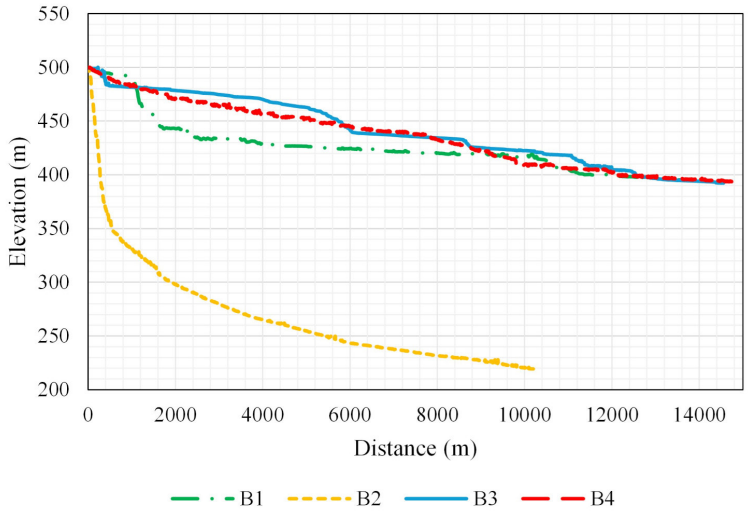


Figure 1. Downstream channel profile.

There were also topobathymetric surveys carried out to properly define the main water channel downstream. The topographies used in the study are of high accuracy and are not considered as a source of uncertainty.

Figure 1 shows the downstream channel profile of each dam. It is possible to notice that while B3 and B4 present relatively uniform slope (~0.7%), B2 presents a highly steep slope (~24%) in the first 600 m, followed by an average slope of 2.7%. The slope of B1 is 0.8% in average, despite in some areas it reaches more than 5%.

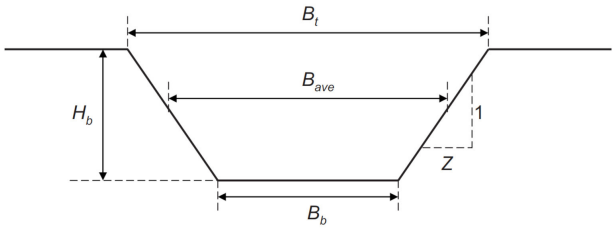


Figure 2. Overtopping and piping breach geometry (Xu & Zhang, 2009).

2.3 Breach parameters and hydrographs

The range of variation expected for breaches considering piping and overtopping failure was evaluated through the methodology presented by Froehlich (2008). The methodology considers that the breach has trapezoidal geometry, which is a usual assumption (Xu & Zhang, 2009; Von Thun & Gillette, 1990; MacDonald & Langridge-Monopolis, 1984), as shown in Figure 2. Froehlich (2008) propose equations to predict width, formation time and side slopes of breaches for overtopping and piping. He also presents the variance expected for the parameters.

In the present study, it was considered that the height of the breach is always the dam's height and is not an evaluated variable. Variable considered were breach width, side slopes and formation time. The expected variation for the breach parameters, considering the information presented by Froehlich (2008) is presented in Table 2. Note that for dams B2 and B3, both the minimum and average values would result in

negative values, meaning that the breach would be triangular and would not extend to the bottom of the valley. However, to maintain the premise of always considering the breach developing to the bottom of the valley and being trapezoidal, a minimum value of 5 m is considered for bottom width (B_b).

For piping failure mode, another required parameter is the elevation from which it is considered that the process is initiated.

With the information presented in Table 2, the expected variation in the peak flow of piping and overtopping failure hydrograph was evaluated using Monte Carlo method probabilistic analysis through a function included in HEC-HMS (v4.12) software (U.S. Army Corps of Engineers, 2024).

In all cases, it was considered that the volume stored at the time of failure is the maximum reservoir volume (tailings + water up to the crest) and that the breach develops in a sinusoidal function. A total of 1000 combinations of breach parameters were simulated for each failure mode, considering that the parameters have a normal distribution. Froehlich (2008) indicates that parameters variation is represented by t-student distribution. However, since t-student is a generalization of normal distribution, for the sake of statistical analysis considering 1000 samples, there is no prejudice in using normal distribution. For the elevation of piping, it was considered that it could vary from the lowest point of the foundation to 2/3 of the height of the dam. The average value considered was the average elevation within the range between the lowest point and the limit of 2/3 of the height of the dam.

To check if 1000 simulations were sufficient to stabilize the process, a plot of the average value of peak flow was prepared to each dam and to each failure mode. Figure 3 presents the average peak flow for overtopping for B1. For all failure modes (overtopping and piping) and for all dams, the average peak flow was stabilized well before 1000 simulations, which means that a great number of simulations should return the same statistical result.

After performing the Monte Carlo simulations, a cumulative plot of peak flow was prepared for each dam and for each failure mode, as illustrated in Figure 4. Three peak flows were selected: peak flow of 50% exceedance probability, peak flow of 16% exceedance probability and peak flow of 5% exceedance probability. These exceedance probabilities were used because 50% represents what should be expected using the equations proposed by Froehlich (2008), 16% is the average plus 1 standard deviation and 5% is a usual recommendation to cover uncertainties, as indicated by Martin et al. (2022).

After selecting the peak flow for each failure mode and each dam, the parameters combination which resulted on the flows were picked from the statistical database and a specific failure hydrograph for each case was defined. The failure hydrographs were also defined using HEC-HMS (v4.12). Summary of breach parameters and peak flow obtained using the aforementioned approach are indicated on Table 3 and Table 4.

For liquefaction, currently there is no methodology to predict breach geometry and formation time. Since liquefaction results in a very quick volume mobilization, the standard practice is to consider that breach geometry is given by the valley geometry, which means that all the dam is mobilized. Regarding formation time, normally it is considered to occur instantaneously. The previously mentioned approach is the one indicated in resolution ANM 95/2022 (ANM, 2022).

Considering the particularities of liquefaction, a single breach hydrograph was defined to each dam. The hydrographs were computed through a numerical model run in Riverflow2D (v8.15.02) software (Hydronia, 2025), where at time zero all the reservoir volume is at static equilibrium and at the first time step, it can flow driven by gravity.

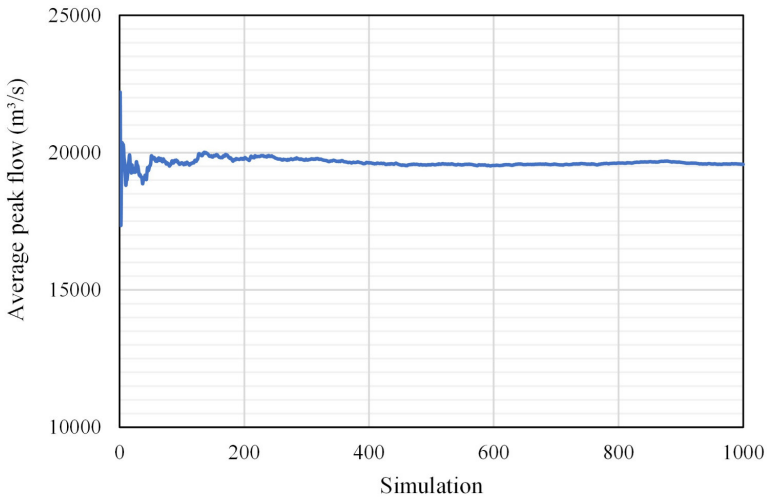


Figure 3. Average peak flow for overtopping for B1.

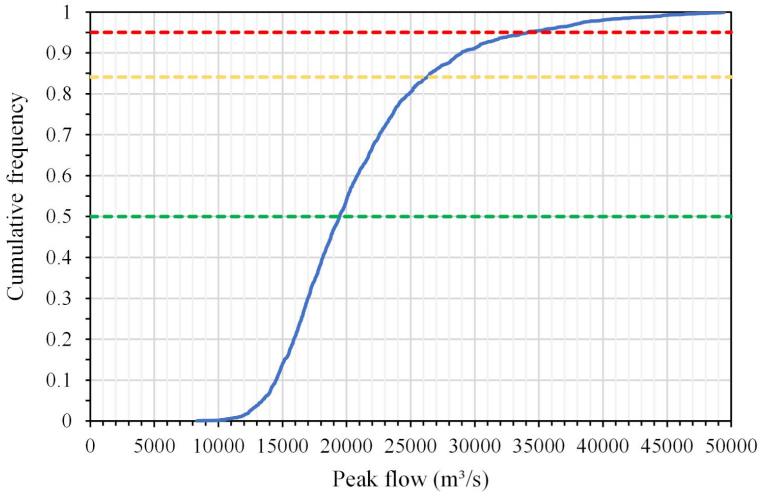


Figure 4. Cumulative frequency for overtopping peak flow resulting from Monte Carlo analysis in B1.

Table 3. Overtopping breach parameters.

Dam	Cumulative frequency	Peak flow (m³/s)	B_b (m)	t_f (h)	*Zl* (H:1)	*Zr* (H:1)
B1	95	34.092	48.713	1.092	1.024	1.008
	84	26.272	42.136	1.697	0.863	2.513
	50	19.444	32.653	2.415	1.989	1.221
B2	95	3.041	17.560	0.369	1.358	0.319
	84	2.601	24.200	0.461	0.583	0.664
	50	2.036	34.466	0.647	0.788	0.340
B3	95	48.856	53.343	0.670	2.414	1.653
	84	41.323	24.698	0.684	1.155	0.583
	50	32.608	94.378	1.132	1.560	1.598
B4	95	2.723	6.713	0.344	0.568	3.551
	84	2.339	5.861	0.443	2.807	2.911
	50	1.585	9.716	0.689	2.312	1.564

Table 4. Piping breach parameters.

Dam	Cumulative frequency	Peak flow (m³/s)	B_b (m)	t_f (h)	*Zl* (h:1)	*Zr* (h:1)	Piping elevation (m)
B1	95	34.401	39.682	1.111	0.439	0.713	506.13
	84	29.094	46.999	1.677	0.676	0.601	521.55
	50	22.413	38.276	2.460	2.066	1.884	535.14
B2	95	4.534	5.424	0.425	1.779	0.995	524.71
	84	3.772	9.377	0.415	1.123	1.033	535.33
	50	2.784	9.620	0.692	1.421	0.566	540.00
B3	95	73.028	87.756	0.801	0.944	0.571	522.44
	84	56.492	79.937	1.272	1.201	0.639	502.44
	50	41.290	43.342	0.660	0.472	0.650	575.94
B4	95	2.922	10.188	0.366	2.014	0.305	509.87
	84	2.398	16.557	0.454	0.643	1.365	513.15
	50	1.792	10.431	0.611	0.786	1.326	515.60

Legend: B_b = breach base width; t_f = time to failure, Z_l = breach left slope; Z_r = breach right slope.

The only constraint to flow is the downstream topography. A boundary condition of open flow was applied just downstream the toe of the dam, and the hydrograph was computed just before the boundary condition. Table 5 summarizes liquefaction peak flow obtained for each dam. Liquefaction hydrographs were defined for all dams considering that flowing fluid is water. Notwithstanding it was possible in these simulations to consider different rheological models, to keep compatibility with hydrograph defined for other failure modes, just water flow was considered.

2.4 Rheological parameters

For B1, rheological parameters were defined based on vane rheometer tests performed on tailings sampled from the dam reservoir. With test data, three different rheological curves for yield stress and dynamic viscosity were defined: an upper limit, a lower limit and an average curve. Upper limit curve was defined to cover 95% of test data and lower curve was defined to cover 5% of test data.

For B2, B3 and B4, instead of using specific rheological parameters, a database composed by 1162 vane rheometer tests performed in Fugro laboratory in sediments and iron ore tailings sampled from 145 tailings dams in Brazil was used (Fugro, personal communication, 2025). These data lie between the range of data presented by Julien (2010). The same concept of upper and lower limit curves was applied for Fugro lab data.

Figure 5 shows rheological curves for B1 data and Figure 6 shows results of Fugro data. Figure 7 shows Fugro data plotted over data presented by Julien (2010). One can see that there is an important scatter for yield stress and viscosity for tailings and sediments tested by Fugro and that the scatter is similar to that indicated by Julien (2010).

2.5 Manning coefficient

Manning coefficient variation was also evaluated. Two sets of values were considered in the study. The first set is the one used normally in hydraulic analysis and the second is an upper limit. The values used are in accordance with range of variation presented by Ball et al. (2019) and Chow et al. (1988) and are indicated in Table 6.

Table 5. Liquefaction peak flow.

Dam	Peak flow (m^3/s)	Time to peak flow (s)
B1	139,650	180
B2	57,210	9
B3	403,100	3
B4	38,260	3

Table 6. Manning coefficients (after Ball et al., 2019; Chow et al., 1988).

Region	Base	Upper limit
Waterways/channels	0.025	0.035
Thick vegetation	0.080	0.120
Light bush and weeds	0.040	0.060

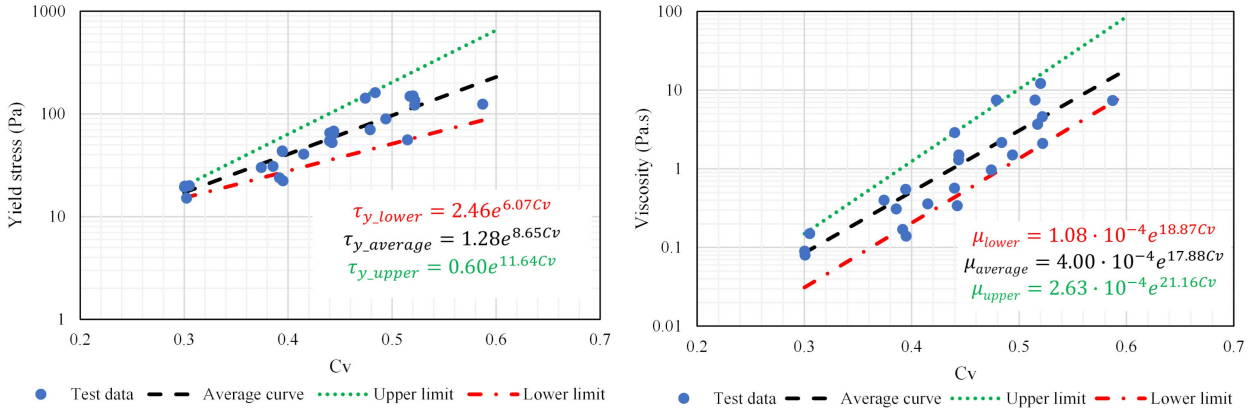


Figure 5. B1 rheological parameters.

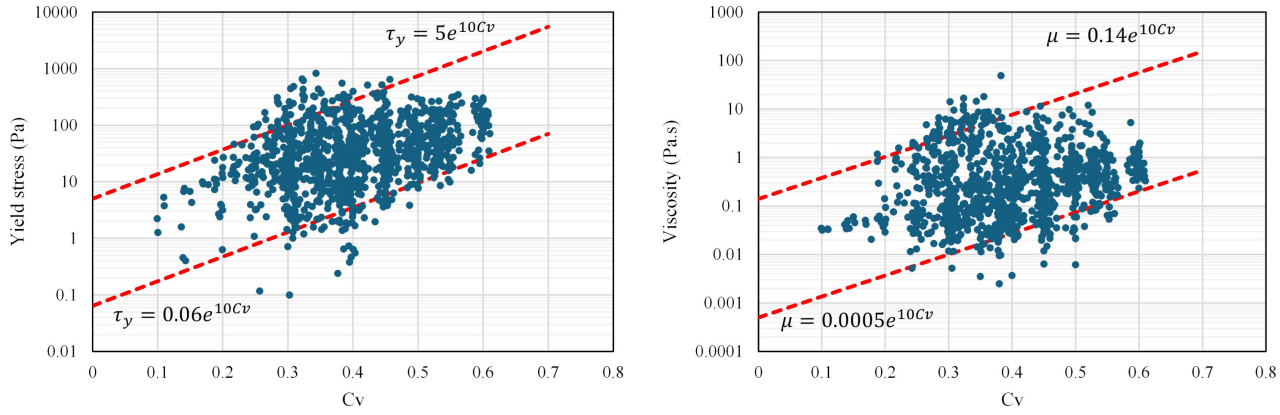


Figure 6. Fugro lab test data (Fugro, personal communication, 2025).

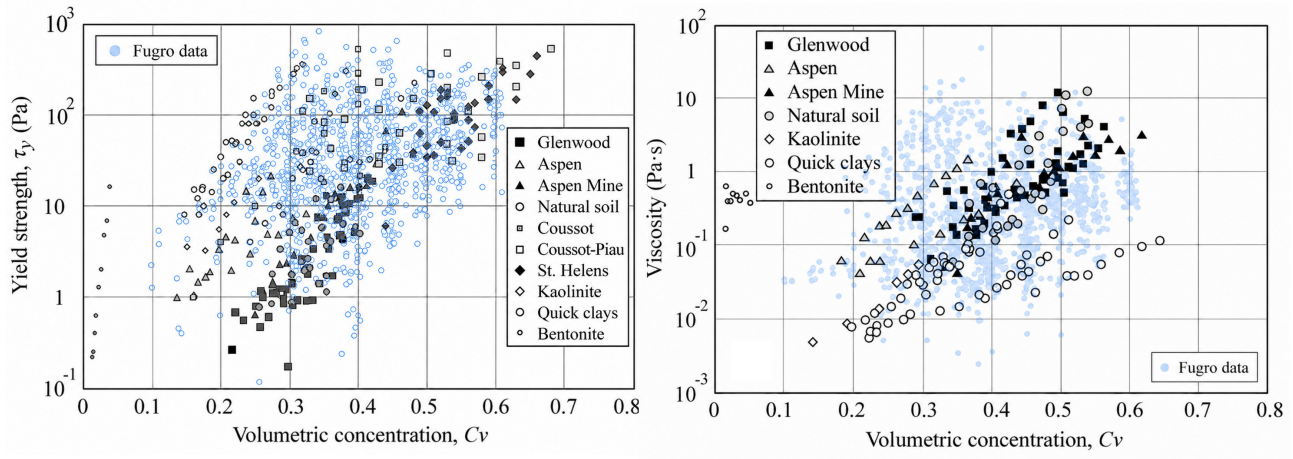


Figure 7. Fugro data compared to data presented by Julien (2010) (Adapted from Julien, 2010).

2.6 Breach runout

Breach runout analysis was performed using Riverflow2D (v8.15.02) (Hydronia, 2025), with Mud and Tailings module. For all cases, variable properties were used. It means that rheological parameters are not constant in time and space during numerical simulation.

Rheological properties vary according to tailings mixture with water during runout. For each dam a constant water flow for 100 years flood was maintained in the main downstream channel. As the tailings flow downstream, they mix with water and the solids volumetric concentration decreases. Yield stress and viscosity also decrease, following the rheological curve associated.

For dam B1, a specific field evaluation, based on sampling, resulted in solids volumetric concentration (*Cv*) variation between 0.42 and 0.47. For the minimum and maximum *Cv* (0.42 and 0.47), three rheological curves (Figure 5) were associated to each failure mode and hydrograph. In addition, a simulation considering tailings as Newtonian fluid with water parameters associated with base Manning coefficient was performed, as well as a simulation considering upper limit Manning coefficient. These combinations resulted in 56 simulations. Table 7 summarizes simulations performed for dam B1.

For dams B2, B3 and B4, in a way to extrapolate results, simulations were not performed using tailings rheology specific for each dam. It was decided to consider minimum and maximum *Cv* of 0.30 and 0.45, respectively. These values are in the range of mud flood (CDA, 2021) and are also in the range normally found in tailings dam in Brazil, where hydraulic disposal was used. For minimum *Cv* (0.30), rheological parameters were selected associated with lower limit curves from Fugro lab data (Figure 6). Maximum *Cv* (0.45) was associated with upper limit curves from Fugro lab data (Figure 6). Simulations were also performed considering Newtonian fluid with water parameters, for two cases of Manning coefficients. These combinations resulted in 28 simulations for each dam, as shown in Table 8.

Table 7. Summary of numerical simulations for dam B1.

Failure mode	Hydrograph peak flow cumulative probability	*Cv*	Rheology	Curve	Manning	Scenario
Overtopping	50%	-	Newtonian	Water	Base	G50CV0
		-			Upper	G50MS
		0.42	Non-Newtonian	Lower	Base	G50CV1I
				Average		G50CV1M
				Upper		G50CV1S
		0.47		Lower		G50CV2I
				Average		G50CV2M
				Upper		G50CV2S
	84%	-	Newtonian	Water	Base	G84CV0
		-			Upper	G84MS
		0.42	Non-Newtonian	Lower	Base	G84CV1I
				Average		G84CV1M
				Upper		G84CV1S
		0.47		Lower		G84CV2I
				Average		G84CV2M
				Upper		G84CV2S
	95%	-	Newtonian	Water	Base	G95CV0
		-			Upper	G95MS
		0.42	Non-Newtonian	Lower	Base	G95CV1I
				Average		G95CV1M
				Upper		G95CV1S
		0.47		Lower		G95CV2I
				Average		G95CV2M
				Upper		G95CV2S
Piping	50%	-	Newtonian	Water	Base	P50CV0
		-			Upper	P50MS
		0.42	Non-Newtonian	Lower	Base	P50CV1I
				Average		P50CV1M
				Upper		P50CV1S
		0.47		Lower		P50CV2I
				Average		P50CV2M
				Upper		P50CV2S
	84%	-	Newtonian	Water	Base	P84CV0
		-			Upper	P84MS
		0.42	Non-Newtonian	Lower	Base	P84CV1I
				Average		P84CV1M
				Upper		P84CV1S
		0.47		Lower		P84CV2I
				Average		P84CV2M
				Upper		P84CV2S
	95%	-	Newtonian	Water	Base	P95CV0
		-			Upper	P95MS
		0.42	Non-Newtonian	Lower	Base	P95CV1I
				Average		P95CV1M
				Upper		P95CV1S
		0.47		Lower		P95CV2I
				Average		P95CV2M
				Upper		P95CV2S
Liquefaction	Single	-	Newtonian	Water	Base	LCV0
		-			Upper	LMS
		0.42	Non-Newtonian	Lower	Base	LCV1I
				Average		LCV1M
				Upper		LCV1S
		0.47		Lower		LCV2I
				Average		LCV2M
				Upper		LCV2S

Table 8. Summary of numerical simulations for dams B2, B3 and B4.

Failure mode	Hydrograph peak flow cumulative probability	*Cv*	Rheology	Curve	Manning	Scenario
Overtopping	50%	-	Newtonian	Water	Base	G50CV0
		-			Upper	G50MS
		0.30	Non-Newtonian	Lower	Base	G50CV1
		0.45		Upper		G50CV2
	84%	-	Newtonian	Water	Base	G84CV0
		-			Upper	G84MS
		0.30	Non-Newtonian	Lower	Base	G84CV1
		0.45		Upper		G84CV2
	95%	-	Newtonian	Water	Base	G95CV0
		-			Upper	G95MS
		0.30	Non-Newtonian	Lower	Base	G95CV1
		0.45		Upper		G95CV2
Piping	50%	-	Newtonian	Water	Base	P50CV0
		-			Upper	P50MS
		0.30	Non-Newtonian	Lower	Base	P50CV1
		0.45		Upper		P50CV2
	84%	-	Newtonian	Water	Base	P84CV0
		-			Upper	P84MS
		0.30	Non-Newtonian	Lower	Base	P84CV1
		0.40		Upper		P84CV2
	95%	-	Newtonian	Water	Base	P95CV0
		-			Upper	P95MS
		0.30	Non-Newtonian	Lower	Base	P95CV1
		0.45		Upper		P95CV2
Liquefaction	Single	-	Newtonian	Water	Base	LCV0
		-			Upper	LMS
		0.30	Non-Newtonian	Lower	Base	LCV1
		0.45		Upper		LCV2

In Table 7, each scenario is named after the failure mode (G = overtopping, P = piping, L = liquefaction) and rheology (CV0 = Newtonian fluid, base Manning; MS = Newtonian Fluid, upper Manning; CV1 = Non-Newtonian for Cv = 0.42; CV2 = Non-Newtonian for Cv = 0.47; I = lower bound curve; M = average curve; S = upper bound curve). In Table 8, scenarios are named in a similar way, with difference that CV1 is for Non-Newtonian fluid for Cv = 0.30 and lower bound curves and CV2 is for Non-Newtonian fluid for CV = 0.45 and upper bound curves.

Riverflow2D formulation is based on Shallow Water Equations (SWE). For Non-Newtonian fluids, there are a variety of rheological models to be used. All simulations performed on the present study used the formulation named quadratic.

The SWE equations are indicated below:

$$\frac{\partial(\rho hU)}{\partial t}+\frac{\partial}{\partial x}\left(\rho hU^2+\rho\frac{1}{2}gh^2\right)+\frac{\partial(\rho hUV)}{\partial y}=-\rho gh\frac{\partial z_b}{\partial x}-\tau_{bx} \quad (1)$$

$$\frac{\partial(\rho hV)}{\partial t}+\frac{\partial(\rho hUV)}{\partial x}+\frac{\partial}{\partial y}\left(\rho hV^2+\rho\frac{1}{2}gh^2\right)=-\rho gh\frac{\partial z_b}{\partial y}-\tau_{by} \quad (2)$$

where: h = flow height; U = velocity in x direction; V = velocity in y direction; g = gravity acceleration; z_b = elevation of channel bottom; τ_{bx} = bottom shear stress in x direction; τ_{by} = bottom shear stress in y direction; ρ = fluid density.

Regardless of the rheological model, Equations (1) and (2) differs only for bottom shear stress terms.

For Newtonian fluids, the bottom shear stress is given by Manning equation:

$$\tau_b=\rho g\frac{n^2|U|^2}{h^{1/3}} \quad (3)$$

where: ρ = fluid density; g = gravity acceleration; n = Manning coefficient; u = velocity; h = flow height.

For Non-Newtonian fluids, when quadratic formulation is used, the bottom shear stress is:

CC BY

$$\tau_b = \rho g \frac{n^2 |U|^2}{h^{1/3}} + \tau_y + 3\mu \frac{|U|}{h} \quad (4)$$

where: ρ = fluid density; g = gravity acceleration; n = Manning coefficient; u = velocity; h = flow height; τ_y = yield stress; μ = dynamic viscosity.

In Equation (4), the term $3\frac{|u|}{h}$ is the shear strain ratio. Comparing Equations (3) and (4), one can observe that in quadratic formulation, Bingham rheological parameters are added to Manning equation. This explains why Manning parameters are also necessary to be considered and are indicated on Table 7 and Table 8.

Numerical domains were discretized with triangular mesh. Mesh size varied from 5 m in main channel to 20 m in the edges. This range of mesh size is between what is found to be adequate by Giantomaso (2023). Domain extents were selected to allow a proper definition of self-rescue zone. It means that the extent was long enough to define arrival time in 30 minutes. Table 9 summarizes numerical domains for all dams.

3. Results

Results were evaluated through four hydraulic variables: arrival time, time to peak, maximum velocity and maximum elevation. Arrival time is the time for the runout wave to reach 30 cm compared to the condition before dam failure. Time to peak is the time necessary for the runout wave to reach its maximum height.

To allow a proper comparison between scenarios, hydraulic variable results were taken in points along the main downstream channel, every 250 m for all dams (chainage). Figure 8 illustrates the numerical domain extent and points where results were evaluated for dam B4 (red dots). A similar approach was used for dam B1, B2 and B3.

The influence of rheological parameters in the breach runout for each dam was evaluated by applying the Kruskal-Walis test to the set of results for each hydraulic variable for each failure mode and hydrograph, separately. The Kruskal-Walis test is a non-parametric statistical method used to compare three or more independent groups. It is the non-parametric equivalent to a one-way ANOVA, used when data does not meet the assumption of a normal distribution. The test results were assessed through the associated p value. Considering significance level of 5%, the hypothesis that groups are equal is rejected when p-value is lower than 0.05.

It means that, for each hydraulic variable, for the same failure mode and same hydrograph, the test result indicates whether different rheological parameters lead to different sets of results. The set of results considered were the results measured at each chain (250 m apart) along the main downstream channel. To maintain compatibility between all dams, data sets were taken up to 10 km downstream for Kruskal-Walis tests.

Table 9. Summary of numerical domain.

Dam	Downstream domain extent (km)	Total mesh elements	Mesh average size (m)	100 years flood flow (m³/s)
B1	13.5	156578	15.0	70
B2	10.3	72822	8.6	29
B3	15.0	137946	12.2	124
B4	15.2	157697	7.8	85

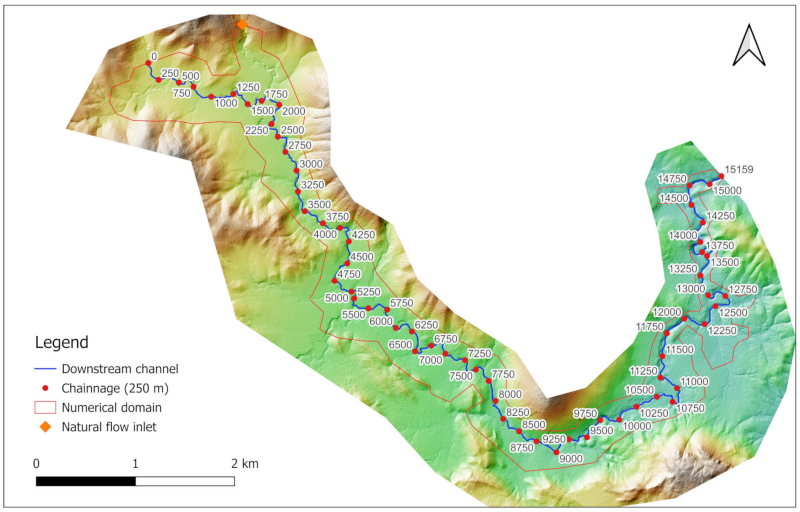


Figure 8. Numerical domain and results evaluation points for dam B4.

To evaluate the effect of different hydrographs and different failure modes, the Kruskal-Walis test was also applied to data sets of simulations considering Newtonian behavior, for base values of Manning coefficient.

To evaluate the effect of rheological parameters and different failure modes and hydrographs on runout area, differences in the runout footprint area were also evaluated. Initially, the variation in area was calculated for the set of results for the same failure mode and same hydrographs. This evaluation indicates the influence of rheological parameters in the runout footprint. Afterwards, results for different failure modes and different hydrographs were compared to the results obtained for overtopping, for peak flow cumulative probability of 50%, always considering Newtonian fluid, for base Manning. It allows the evaluation of the influence of hydrographs and failure modes. In all cases, the footprints downstream extent were also considered up to 10 km downstream. This consideration means that the area variation in footprint is due to lateral variation.

Finally, variation in ZAS extent for each dam was also assessed, considering definition indicated in resolution ANM 95/2022.

Table 10 to 13 present p-value for Kruskal-Walis tests for all dams. It can be seen that for all dams, rheological parameters variation (columns G50, G84, G95, P50, P84, P95 and L) resulted in no significant variation in arrival time, time to peak, maximum height and maximum velocity. In fact, variation observed is, in general, in the range of 5 to 10%.

In contrast, different hydrographs resulted in significant variation in arrival time and time to peak for all dams. For maximum height and maximum velocity, difference was not significant for all dams.

Regarding ZAS extent definition, which is given by 10 km of extent for 30 minutes wave arrival time, for dam B1, for all cases of piping and overtopping, arrival time in 30 minutes resulted in less than 10 km. For liquefaction, regardless rheology, arrival time in 30 minutes was around 12.5 km. For dams B2 and B3, results were similar.

Table 10. P-value for Kruskal-Walis test for arrival time results.

Dam	G50	G84	G95	P50	P84	P95	L	Hydrograph variation (Newtonian Fluid)
B1	0.9997	0.9997	0.9996	0.9997	0.9996	0.9999	0.9999	0.0000
B2	0.9851	0.9875	0.9866	0.9850	0.9867	0.9869	0.9845	0.0001
B3	0.9233	0.9226	0.9217	0.9238	0.9276	0.9289	0.9473	0.0000
B4	0.7644	0.7610	0.7736	0.7531	0.7558	0.7567	0.7261	0.0000

Table 11. P-value for Kruskal-Walis testo for time to peak results.

Dam	G50	G84	G95	P50	P84	P95	L	Hydrograph variation (Newtonian Fluid)
B1	0.3378	0.5989	0.6740	0.5042	0.6306	0.6896	0.9983	0.0000
B2	0.9411	0.9699	0.9697	0.9678	0.9649	0.9706	0.9692	0.0000
B3	0.8253	0.8636	0.9095	0.8649	0.9280	0.9279	0.8051	0.0000
B4	0.1909	0.2276	0.2676	0.2041	0.2453	0.2626	0.2433	0.0000

Table 12. P-value for Kruskal-Walis test for maximum velocity results.

Dam	G50	G84	G95	P50	P84	P95	L	Hydrograph variation (Newtonian Fluid)
B1	0.9855	0.9155	0.9253	0.9286	0.9342	0.9479	0.9999	0.0000
B2	0.8204	0.8555	0.8000	0.8018	0.8001	0.8009	0.8372	0.0812
B3	0.2707	0.2916	0.2484	0.2798	0.2718	0.2747	0.4443	0.0096
B4	0.2571	0.2821	0.2626	0.1816	0.1809	0.1902	0.2934	0.1834

Table 13. P-value for Kruskal-Walis test for maximum height results.

Dam	G50	G84	G95	P50	P84	P95	L	Hydrograph variation (Newtonian Fluid)
B1	0.9966	0.9665	0.9707	0.9955	0.9994	0.9992	1.0000	0.0000
B2	0.8761	0.9322	0.8088	0.8930	0.8577	0.8787	0.8568	0.0001
B3	0.3898	0.5274	0.6085	0.5388	0.6758	0.6780	0.4211	0.5374
B4	0.2083	0.1670	0.1768	0.5766	0.4267	0.4271	0.0837	0.0795

Legend: G50 = overtopping failure mode, hydrograph with 50% peak flow cumulative probability; G84 = overtopping failure mode, hydrograph with 84% peak flow cumulative probability; G95 = overtopping failure mode, hydrograph with 95% peak flow cumulative probability; P50 = piping failure mode, hydrograph with 50% peak flow cumulative probability; P84 = piping failure mode, hydrograph with 84% peak flow cumulative probability; P95 = piping failure mode, hydrograph with 95% peak flow cumulative probability; L = liquefaction failure mode. Hydrograph variation (Newtonian Fluid) = test for different failure mode and hydrographs, always considering Newtonian fluid.

CC BY

Table 14. Runout footprint variation for a single failure mode and single hydrograph.

Dam	G50	G84	G95	P50	P84	P95	L
B1	2.66%	2.92%	2.44%	2.51%	2.74%	2.57%	1.12%
B2	2.56%	0.68%	3.30%	3.20%	3.00%	2.19%	3.42%
B3	2.59%	1.99%	1.71%	2.05%	1.87%	1.64%	3.31%
B4	6.99%	6.63%	6.50%	5.55%	7.10%	6.86%	9.34%

Table 15. Runout footprint variation for Newtonian fluid simulation for different hydrographs compared to overtopping.

Dam	G50CV0	G84CV0	G95CV0	P50CV0	P84CV0	P95CV0	LCV0
B1	-	6.61%	12.70%	2.65%	7.13%	9.88%	29.00%
B2	-	7.80%	13.18%	7.65%	17.22%	21.34%	64.24%
B3	-	3.28%	4.30%	3.43%	6.66%	9.24%	20.50%
B4	-	3.07%	5.43%	0.43%	2.75%	6.37%	17.15%

Legend: B_b = breach base width; B_{ave} = breach average width; B_t = breach top width; H_b = breach height; Z = breach side slope.

Only liquefaction resulted in change in ZAS extent. In dam B2, for liquefaction, ZAS extent was between 10.0 and 10.25 km. For dam B3, liquefaction ZAS extent varied between 11.25 and 12.25 km. For dam B4, in none of the simulated cases wave arrival time occurred to an extent higher than 10 km.

In respect to runout footprint area, Table 14 presents maximum area variation considering the same failure mode and same hydrograph. It means that area variation is only given by rheological parameters change. All footprint downstream extent was kept in 10 km, to isolate the lateral variation. Results show that rheological parameters had limited effect on lateral extent of runout footprint.

Table 15 present runout footprint area variation, always considering Newtonian fluid, compared to overtopping, for 50% peak flow cumulative probability, which was considered as a base case. Results indicated that different hydrographs lead to area variation higher than rheological parameters. Again, in all cases footprint downstream extent was limited to 10 km. Results show that breach hydrograph does influence footprint area.

4. Summary and conclusions

The present study intended to evaluate the influence of failure mode, breach and rheological parameters on the definition of self-rescue zone (ZAS) and on selected hydraulic variables inside ZAS for tailings dams. For this purpose, four tailings dams of different sizes were selected. All dams store iron ore tailings. Failure mode and breach parameters were evaluated for overtopping, piping and liquefaction. All failure modes were considered for all dams. Breach parameters variation for overtopping and piping was considered according to Froehlich (2008). For overtopping and piping, three different breach hydrographs were selected, each one associated to a peak flow cumulative probability of 50, 84 and 95%, based on Monte Carlo simulations. For liquefaction, a single breach hydrograph was considered.

In defining breach hydrograph, for all cases, Newtonian fluid with water parameters were considered.

Breach runout simulations were performed using variable parameters in Mud and Tailings module of Riverflow2D. A total of 140 breach runout simulations were performed, being 56 for dam B1 and 28 for each of dams B2, B3 and B4.

For dam B1, a specific set of rheological parameters were considered, based of vane rheometer tests performed on tailings sampled from the dam reservoir. For dams B2, B3 and B4, parameters taken from 1162 vane rheometer tests performed in Fugro laboratory in iron ore tailings and sediment were taken. For each dam, simulations were performed considering Newtonian fluid (water parameters) with regular and upper values of Manning coefficient and Non Newtonian fluid (quadratic rheology) for upper and lower expected rheological parameters and regular Manning.

Results were assessed for four hydraulic variables (arrival time, time to peak, maximum velocity and maximum height) every 250 m along the main downstream channel. In addition, lateral variation in runout footprint was also computed. For hydraulic variables, differences between each simulation case were assessed through Kruskal-Walis test over the data set composed of 40 values (250 to 10000 m) for each simulation.

Main findings were:

- For all dams, no significant statistical differences were observed in the hydraulic variables for rheological parameters variation for the same failure mode and hydrograph;
- Statistical differences were observed for arrival time and time to peak for all dams when comparing the effect of different failure modes and hydrographs. Differences were also observed for maximum height and maximum velocity, but not for all dams;
- For the same failure mode and hydrograph, variation in rheological parameters have not influenced downstream extent of ZAS. For overtopping and piping, regardless of rheology or hydrograph, ZAS extent was defined as 10 km. The only variable which influenced ZAS downstream extent was liquefaction as a failure mode;

CC BY

- Lateral variation in runout footprint was limited for the same failure mode and hydrograph, considering variation in rheological parameters. Variations were more expressive when comparing different failure modes and hydrographs, especially liquefaction.

The findings indicated that the breach hydrograph influences the wave runout dynamics more than rheological parameters. Upper values of Manning coefficient produced almost the same variation in results as obtained from rheological parameters.

Results lead to conclusion that, for evaluated conditions, rheological parameters are just one of the variables influencing breach runout, none the most important. A reliable breach runout analysis should address properly failure mode, released volume, breach parameters, downstream topography and Manning coefficient. In absence of specific rheological parameters, literature data could be used, without prejudice, for mud flood cases defined as indicated in CDA (2021).

Declaration of interest

The authors have no conflicts of interest to declare. All co-authors have observed and affirmed the contents of the paper and there is no financial interest to report.

Authors' contributions

Pedro de Carvalho Thá: conceptualization, methodology, analysis, writing – original draft. André Luiz Tonso Fabiani: supervision, writing – review & editing.

Data availability

The datasets of hydraulic variables generated in the course of the current study are available from the corresponding author upon request.

Declaration of use of generative artificial intelligence

This work was prepared without the assistance of any generative artificial intelligence (GenAI) tools or services. All aspects of the manuscript were developed solely by the authors, who take full responsibility for the content of this publication.

List of symbols and abbreviations

g	Gravity acceleration
h	Flow height
n	Manning coefficient
t_f	Breach development time
u	Velocity
z_b	Elevation of channel bottom
ANM	Agência Nacional de Mineração (National Mining Agency, Brazil)
Av	Average
B_{ave}	Breach average width
B_b	Breach base width
B_t	Breach top width
CDA	Canadian Dam Association
Cv	Volumetric concentration
CV0	Newtonian fluid, base Manning
CV1	Non-Newtonian for $Cv = 0.42$
CV2	Non-Newtonian for $Cv = 0.47$
G	Overtopping
H_b	Breach height
I	Lower bound curve
ICOLD	International Comission on Large Dams
L	Liquefaction
M	Average curve
Max	Maximum
Min	Minimum
MS	Newtonian Fluid, upper Manning
P	Piping
S	Upper bound curve
SD	Standard Deviation
SWE	Shallow Water Equations
U	Velocity in x direction
V	Velocity in y direction
ZAS	Zona de Autossalvamento (Self-rescue zone)
Zl	Breach left side slope
Zr	Breach right side slope
μ	Dynamic viscosity
ρ	Fluid density
τ_{bx}	Bottom shear stress in x direction
τ_{by}	Bottom shear stress in y direction
τ_y	Yield stress

References

Agência Nacional de Mineração – ANM. (2022). Resolução ANM nº 95, de 7 de fevereiro de 2022: Consolida os atos normativos que dispõem sobre segurança de barragens de mineração. *Diário Oficial [da] República Federativa do Brasil*, seção 1. Retrieved in July 31, 2026, from https://www.gov.br/anm/pt-br/assuntos/barragens/legislacao/resolucao-no-95-2022.pdf

ABNT NBR 17188. (2024). *Barragens — Ruptura hipotética — Diretrizes*. ABNT, Rio de Janeiro.

Ball, J., Babister, M., Nathan, R., Weeks, W., Weinmann, E., Retallick, M., & Testoni, I. (2019). *Australian rainfall and runoff: A guide to flood estimation: Book 6—Flood hydraulics*. Geoscience Australia.

Brasil. Presidência da República. (1984). Decreto nº 89.817, de 20 de junho de 1984: Estabelece as Instruções Reguladoras das Normas Técnicas da Cartografia Nacional. *Diário Oficial [da] República Federativa do Brasil*, seção 1. Retrieved in July 31, 2026, from https://www.planalto.gov.br/ccivil_03/decreto/1980-1989/d89817.htm

Canadian Dam Association – CDA. (2021). *Technical bulletin: Tailings dam breach analysis*. CDA.

Chow, V.T., Maidment, D.R., & Mays, L.W. (1988). *Applied hydrology*. McGraw-Hill.

Federal Emergency Management Agency – FEMA. (2013). *Federal guidelines for inundation mapping of flood risks associated with dam incidents and failures (FEMA P-946)*. U.S. Department of Homeland Security.

Fernandes, R.B. (2020). *Panorama geotécnico das rupturas de barragens e gestão de risco* (1. ed.). Editora Appris.

Froehlich, D.C. (1995). Embankment dam breach parameters revisited. *Water Resources Engineering*, 1995, 887-892.

Froehlich, D.C. (2008). Embankment dam breach parameters and their uncertainties. *Journal of Hydraulic Engineering (New York, N.Y.)*, 234(22), 2708-2722. https://doi.org/10.1061/(ASCE)0733-9429(2008)134:12(1708).

Froehlich, D.C. (2016). Predicting peak discharge from gradually breached embankment dam. *Journal of Hydrologic Engineering*, 21(11), 04016041. https://doi.org/10.1061/(ASCE)HE.1943-5584.0001424.

Giantomaso, C.E.F. (2023). *Análise de sensibilidade da utilização do software RiverFlow2D na modelagem numérica de ruptura de barragem de rejeitos* [Master's dissertation]. Universidade Federal do Paraná.

Gildeh, H.K., Halliday, A., Arenas, A., & Zhang, H. (2021). Tailings dam breach analysis: A review of methods, practices, and uncertainties. *Mine Water and the Environment*, 40(1), 128-150. https://doi.org/10.1007/s10230-020-00718-2.

Ghahramani, N., Chen, H.J., Clohan, D., Liu, S., Llano-Serna, M., Rana, N.M., McDougall, S., Evans, S.G., & Take, W.A. (2022). A benchmarking study of four numerical runout models for the simulation of tailings flows. *The Science of the Total Environment*, 827, 154245. https://doi.org/10.1016/j.scitotenv.2022.154245.

Ghahramani, N., Adria, D.M., Rana, N.M., Llano-Serna, M., McDougall, S., Evans, S.G., & Take, W.A. (2024). Analysis of uncertainty and sensitivity in Tailings Dam Breach-Runout Numerical Modelling. *Mine Water and the Environment*, 43(1), 87-103. https://doi.org/10.1007/s10230-024-00970-w.

Global Tailings Review. (2020). *Global industry standard on tailings management*. International Council on Mining and Metals.

Hydronia, L.L.C. (2025). *RiverFlow2D (Version 8.15.02)* [Computer software]. Hydronia, LLC.

International Commission on Large Dams – ICOLD. (2011). *Constitution Statuts - Foundation for the United States Constitution*. ICOLD.

International Commission on Large Dams – ICOLD. (2025). *ICOLD incident database Bulletin 99 update: Statistical analysis of dam failures* (Bulletin, No. 188, 1st ed.). CRC Press.

Julien, P.Y. (2010). *Erosion and sedimentation*. Cambridge: Cambridge University Press eBooks. https://doi.org/10.1017/CBO9780511806049

MacDonald, T.C., & Langridge-Monopolis, J. (1984). Breaching charateristics of dam failures. *Journal of Hydraulic Engineering (New York, N.Y.)*, 110(5), 567-586. https://doi.org/10.1061/(ASCE)0733-9429(1984)110:5(567).

Martin, V., Adria, D., Wong, H. (June, 2022). Inundation modelling of non newtonian tailings dam breach outflows. In *Proceedings of the 27th International Congress on Large Dams*. Marseille, France. Retrieved in September 30, 2026, from https://knightpiesold.com/sites/en/assets/File/ICOLD%202022%20-%20Non-Newtonian%20Tailings%20Breach%20Outflows.pdf

Piciullo, L., Storrøsten, E.B., Liu, Z., Nadim, F., & Lacasse, S. (2022). A new look at the statistics of tailings dam failures. *Engineering Geology*, 303, 106657. https://doi.org/10.1016/j.enggeo.2022.106657.

Rana, N.M., Ghahramani, N., Evans, S.G., McDougall, S., Small, A., & Take, W.A. (2021). Catastrophic mass flows resulting from tailings impoundment failures. *Engineering Geology*, 292, 106262. https://doi.org/10.1016/j.enggeo.2021.106262.

Stark, T.D., Moya, L., & Lin, J. (2022). Rates and causes of tailings dam failures. *Advances in Civil Engineering*, 2022(1), 7895880. https://doi.org/10.1155/2022/7895880.

U.S. Army Corps of Engineers. Hydrologic Engineering Center. (2024). *HEC-HMS Hydrologic Modeling System (Version 4.12)* [Computer software]. U.S. Army Corps of Engineers.

Von Thun, J.L., & Gillette, D.R. (1990). *Guidance on breach parameters* [Unpublished internal memorandum]. U.S. Department of the Interior, Bureau of Reclamation.

Walsh, A., McDougall, S., Evans, S.G., & Take, W.A. (2021). Effect of upstream dam geometry on peak discharge during overtopping breach in noncohesive homogeneous embankment dams; implications for tailings dams. *Water Resources Research*, 57(12), e2020WR029358. https://doi.org/10.1029/2020WR029358.

West, M., Morris, M., & Hassan, M. (2018). A guide to breach prediction. *Dams & Reservoirs*, 28(4), 150-152. https://doi.org/10.1680/jdare.18.00031.

Xu, Y., & Zhang, L.M. (2009). Breaching parameters for earth and rockfill dams. *Journal of Geotechnical and Geoenvironmental Engineering*, 135(12), 1957-1970. https://doi.org/10.1061/(ASCE)GT.1943-5606.0000162